Supporting Information

Proctor et al. 10.1073/pnas.1516725113

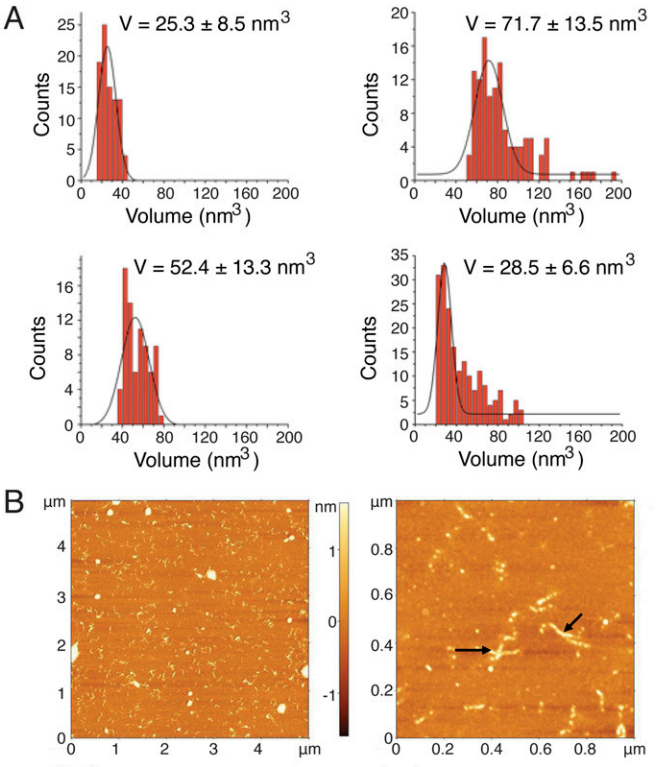

Fig. S1. Volume distributions of SOD1 oligomers demonstrate trimeric stoichiometry. (*A*) At pH 3.5, the volume (V) distribution of SOD1 monomer is narrow, with its peak centered at 25.3 nm^3 (*Left*), whereas the volume distribution of SOD1 oligomer is broad, with its peak centered at 71.7 nm^3 (*Right*). Notably, the volume of oligomer is approximately triple the volume of monomer, denoting that the SOD1 oligomer is trimeric. (*Left*) At pH 7.4, the peak of the dimeric volume distribution is centered at 52.4 nm^3. (*Right*) Oligomeric volume distribution, although featuring a broad tail leading up to oligomeric values, has a peak centered at 28.5 nm^3, comparable to the SOD1 monomer at pH 3.5, denoting that the SOD1 oligomer is primarily dissociated at pH 7.4. Errors are ±SD. Data were obtained with regular AFM of dried samples. (*B*) Using AFM, under trimer-stabilizing conditions, we observe small populations of short, insoluble fibrils with a molecular mass >600 kDa: 5 μm × 5 μm (*Left*) and 1 μm × 1 μm (*Right*) images. The color bar denotes feature height. Arrows indicate fibrils. Data and images were obtained with AFM of dried samples.

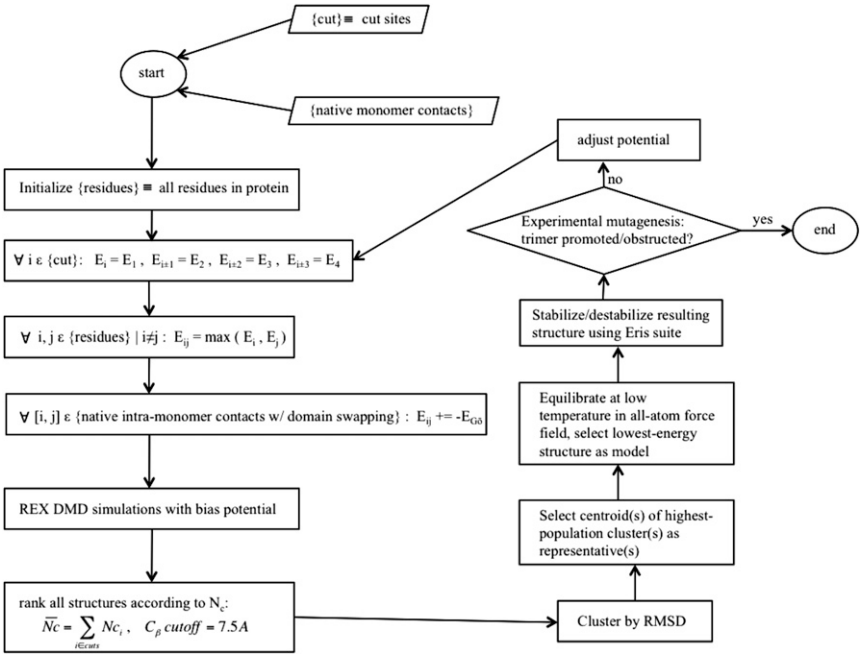

Fig. S2. Schematic diagram for structural modeling of metastable protein oligomers. The procedure for deriving a bias potential using experimental constraints from limited proteolysis is illustrated. The term {cut} is the set of residues at which a proteolytic cut is made. E_1, E_2, E_3, and E_4 are the repulsive potentials applied to (*i*) the residues that are the site of proteolytic cuts, (*ii*) residues 1 removed in sequence from cut sites, (*iii*) residues 2 removed in sequence from cut sites, and (*iv*) residues 3 removed in sequence from cut sites. E_{ij} are the interresidue interaction energies applied when residues are within contact range. $E_{G\bar{o}}$ is the interaction energy assigned to native contacts that are in contact range. N_c is the average number of contacts made by each cut site residue.

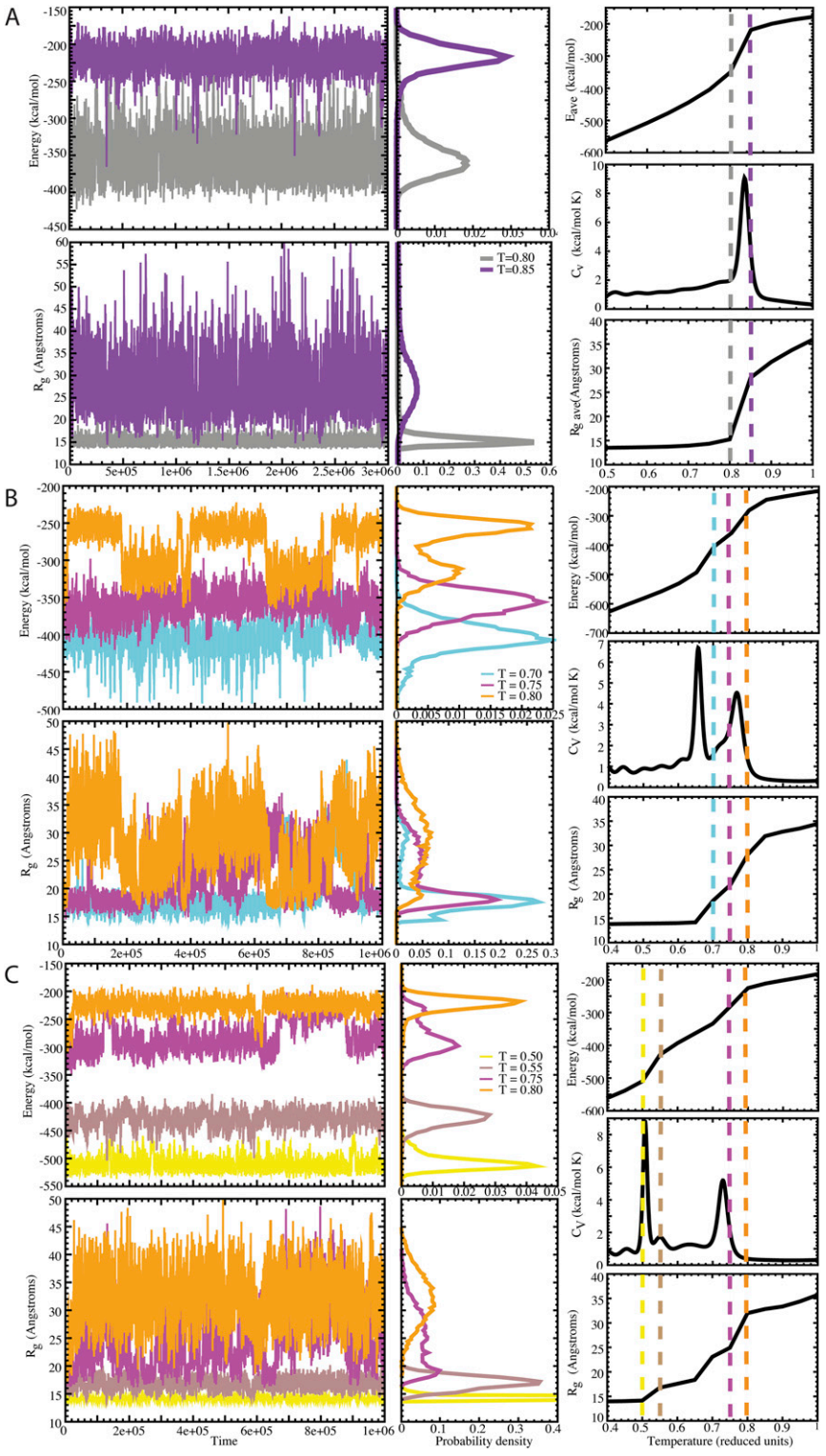

Fig. S3. Folding of SOD1 monomer with various values of λ. (*A*) $\lambda = 0$: SOD1 monomer folding features two distinct states with no folding intermediates. Transitions in energy and the radius of gyration are sharp and well-defined. Trajectories from T = 0.80 and T = 0.85 are located at the transition, and exhibit flipping between folded and unfolded structures. (*B*) $\lambda = 0.66$: SOD1 monomer folding features distinct intermediate states. Transitions in energy and the radius of gyration remain well-defined. Trajectories from T = 0.70, T = 0.75, and T = 0.80 are located at the transition, and exhibit flipping between states. (*C*) $\lambda = 0.99$: SOD1 monomer folding features distinct intermediate states, with a greater separation in energy at $\lambda = 0.66$. Transitions in energy and the radius of gyration are well-defined. Trajectories from T = 0.50 and T = 0.55 and from T = 0.75 and T = 0.80 are located at the transitions, and exhibit flipping between two respective states. C_V, heat capacity at constant volume.

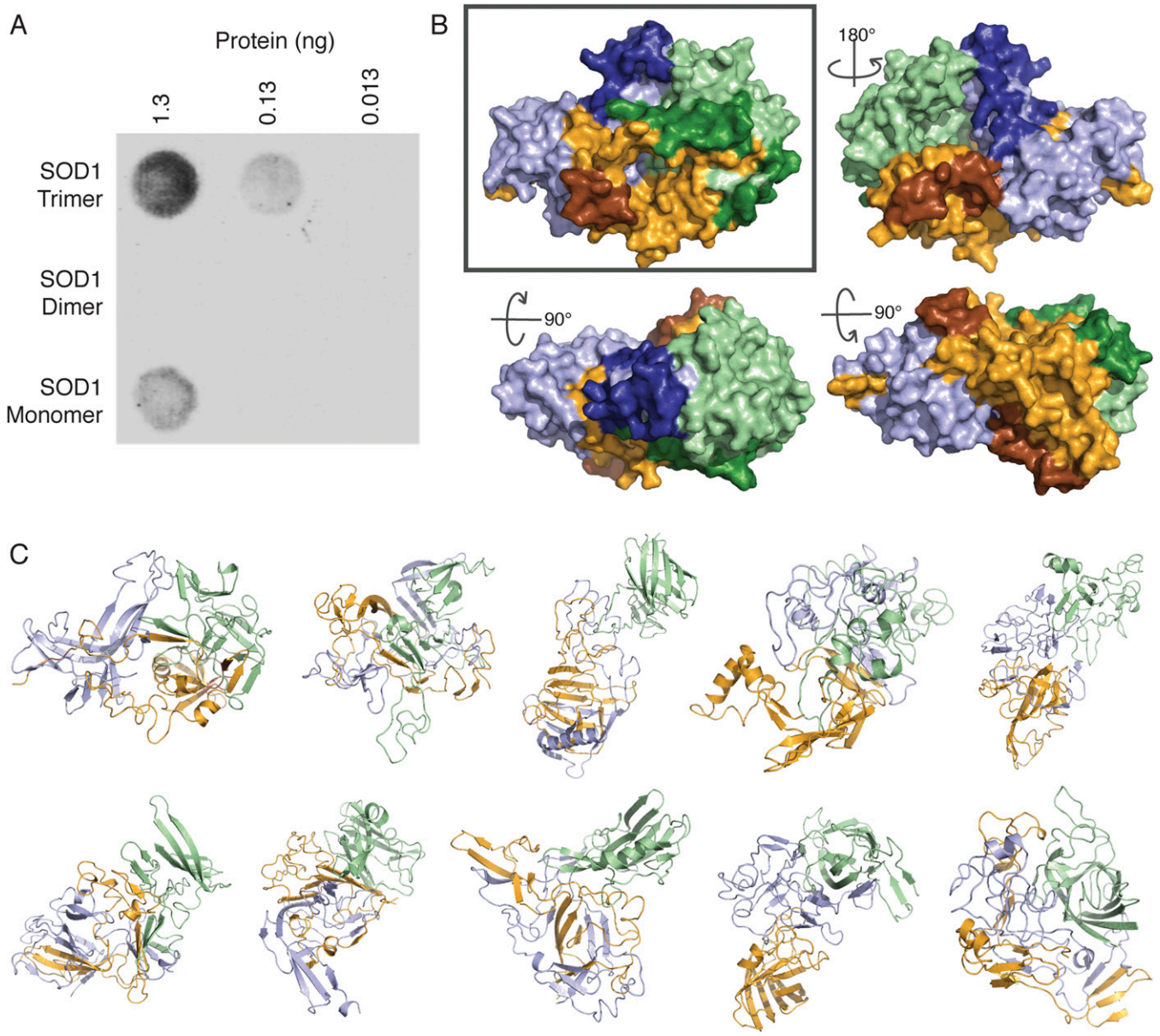

Fig. S4. Toxic epitope exposed on SOD1 trimer surface. Ensemble of SOD1 trimer models. (*A*) Conformational Ab C4F6, which binds several disease-associated species of SOD1 (16), selectively binds to WT SOD1 trimer at various concentrations, but does not bind to native WT type SOD1 dimer and exhibits minimal binding to WT SOD1 monomer. (*B*) Recently identified epitope of the C4F6 Ab (16, 18) is exposed on the surface of our SOD1 trimer model. Individual monomers are depicted in pale green, bright orange, and light blue; residues comprising the C4F6 epitope are highlighted in darker colors: forest, brown, and deep blue, respectively. Rotation angles describe the transformation from the "front" (*Upper Left*), such that the structures represent the "back" (*Upper Right*), "top" (*Lower Left*), and "bottom" (*Lower Right*). The C4F6 Ab has been shown previously to bind WT and disease-linked mutant SOD1 trimer at physiological pH (15). In addition to experimental data from limited proteolysis, the exposure of the C4F6 epitope further verifies our model, as well as providing support for the toxicity of SOD1 trimer. (*C*) Replicate SOD1 trimer models resulting from 10 independent repetitions of our protocol (Fig. S3) feature significant variation in tertiary and quaternary structure. Models vary in the degree of domain swapping, as well as in the amount of native tertiary structure maintained in each monomer. We note that despite differences in tertiary and quaternary structure of the 10 SOD1 trimer models, a high level of consensus on the identity of residues involved in trimeric interface interactions is maintained, with at least 77% and as much as 94% identity in interface residue identity between any two models.

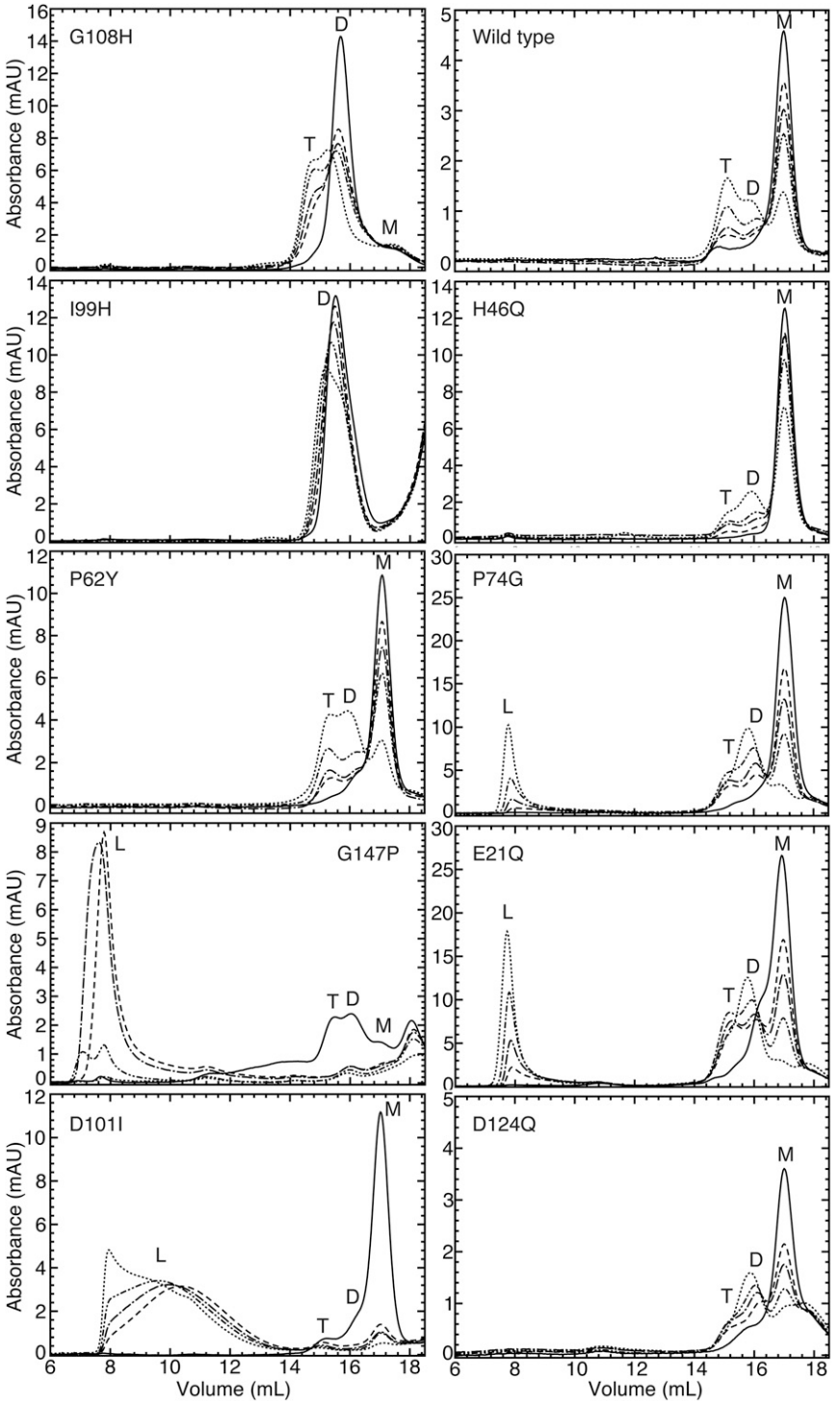

Fig. S5. Designed mutations verify the model and demonstrate control of SOD1 aggregation. Mutations to trimer interface residues are designed to stabilize or destabilize SOD1 trimer but to have no effect on SOD1 monomer or dimer. $\Delta\Delta G_{mut}$ for the trimer, native dimer, and native monomer structures can be found in Fig. 3. Aggregation time courses were measured for each mutant after incubation at physiological concentration (30 μM) and 37 °C for 0 h (solid line), 2 h (– –), 4 h (– – •), 8 h (– • •), or 24 h (• •). The aggregation of apo-WT SOD1 is shown for comparison, with trimer (T), dimer (D), monomer (M), and large aggregate (L) peaks labeled when present. We find that the G108H, I99H, and P62Y mutations, predicted to be destabilizing to the SOD1 trimer, result in smaller populations of trimer than WT, shifting the SOD1 population toward dimer and monomer formations. The G147P and D101I mutations, also predicted to destabilize SOD1 trimer, result in no or very little detectable SOD1 trimer after 24 h, but instead increased populations of large aggregates, especially in G147P-SOD1. In four additional mutants that we predict to be trimer-stabilizing, H46Q-SOD1, D124Q-SOD1, P74G-SOD1, and E21Q-SOD1, we observe the formation of trimer that is overcome by a nonnative extended dimer species (Fig. S6), which (as discussed in the main text) we could not predict computationally. mAU, milli-absorbance units.

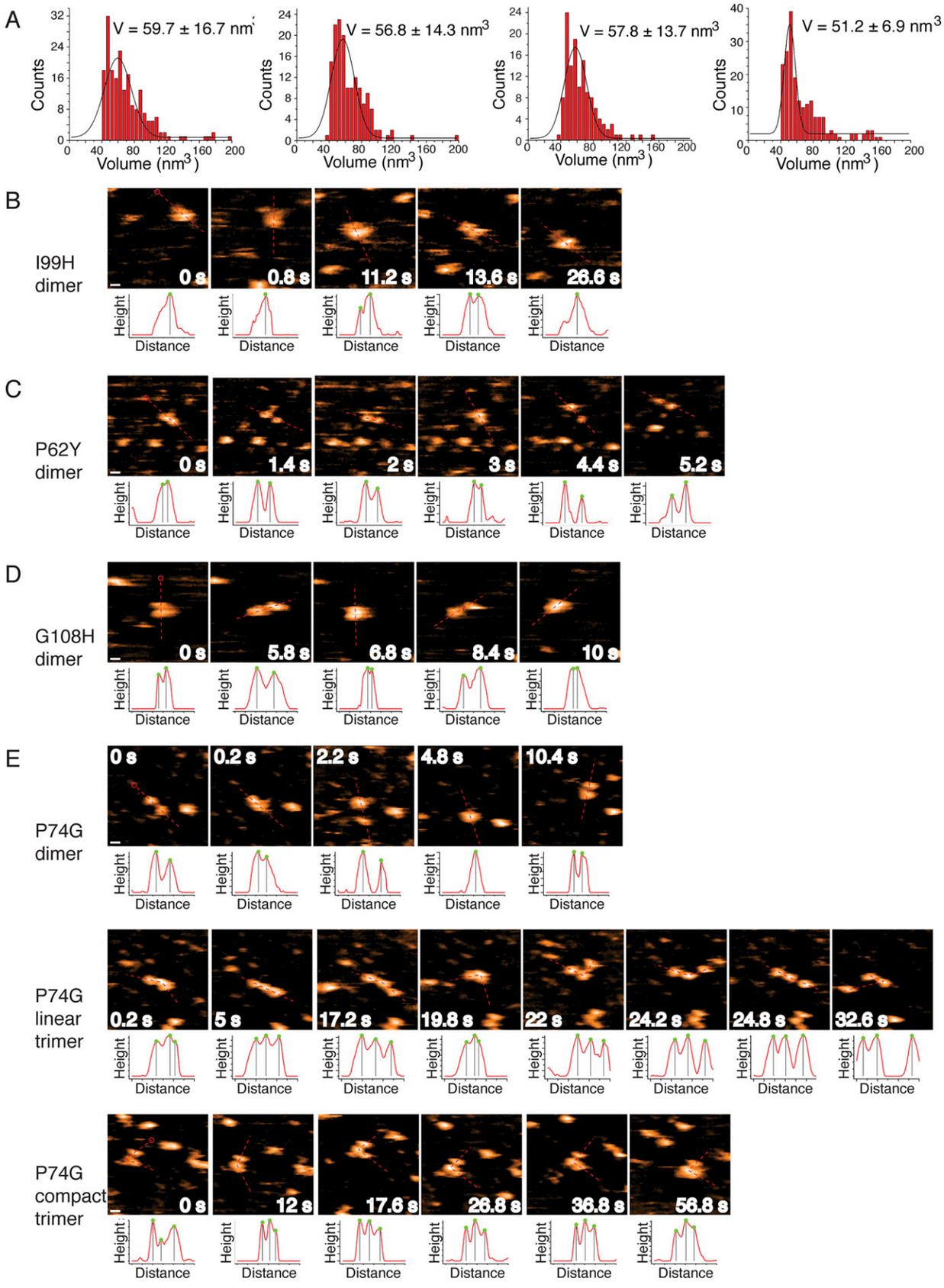

Fig. S6. Mutations to SOD1 trimer interfaces stabilize formation of nonnative extended dimer conformations. (*A*) Volume distributions of (left to right) I99H, P74G, P62Y, and G108H after 24 h of aggregation at 30 μM SOD1 at 37 °C indicate dominance of a nonnative dimer species. Solid lines are Gaussian fits, with most probable volume designated. Errors are ±SD. (*B*) I99H-SOD1, a trimer-destabilizing mutant, exists almost exclusively as an extended dimer, as demonstrated by HS-AFM images. (*C*) P62Y-SOD1, a trimer-destabilizing mutant, exists as an extended dimer, as demonstrated by HS-AFM images. (*D*) G108H-SOD1, a trimer-destabilizing mutant, exists as an extended dimer with a small trimeric population (not shown), as demonstrated by HS-AFM images. (*E*) P74G-SOD1, a trimer-stabilizing mutant, exists as an extended dimer and linear or compact trimer. In *B*–*E*, the scan area is 50 nm × 50 nm. (Scale bar: *B*–*E*, 5 nm.) Dashed lines on the image represent the 1D cross-section used for height profiling below each image, with red circles indicating the initial point of measurement. Green dots on the height profiles indicate peak positions, with the distance between the two gray lines representing the distance of two adjacent subunits. Data were obtained with regular AFM imaging of dried samples.

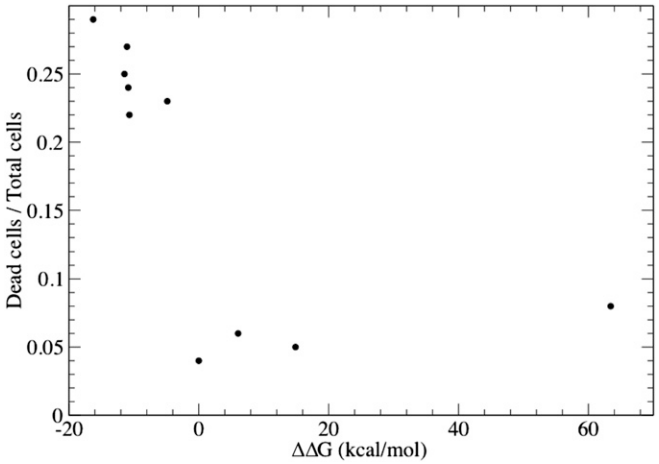

Fig. S7. Stabilization of trimer correlates with cell death. The size of the SOD1 trimer population is proportional to the stability of that species in relation to other SOD1 species. We find that the stability of the SOD1 trimer is highly indicative of the incidence of cell death, with the stability of the mutants corresponding to cell death with a *P* value of 0.0476 (as calculated from the Fisher test) when all points are included. With removal of the outlier P62Y-SOD1, which mutation is extremely destabilizing at +62 kcal/mol (Fig. 3), the *P* value of the relation between SOD1 trimer stability and cell death becomes 0.001.

Table S1. ALS-linked mutations stabilize SOD1 trimer

Original AA	Residue	Mutation	$\Delta\Delta G_T$	$\Delta\Delta G_D$	$\Delta\Delta G_M$
A	4	S	−9.51	5.728	−2.256
A	4	T	−12.996	9.072	−2.741
A	4	V	−4.844	8.659	0.62
V	7	E	−3.711	12.873	−4.104
L	8	Q	−1.052	12.078	1.658
L	8	V	−6.481	1.131	4.981
G	10	R	15.741	20	2.724
G	10	V	16.084	20	−2.917
G	12	R	−2.968	20	2.05
G	16	S	−5.171	19.269	6.765
N	19	S	−7.77	2.324	−2.961
E	21	K	−10.52	4.360	1.798
Q	22	L	−11.609	4.624	−6.264
G	37	R	−7.104	7.437	22.474
L	38	V	−2.494	−0.416	6.446
G	41	D	2.055	0.098	−3.873
G	41	S	−1.33	1.254	−1.104
H	46	R	−1.715	7.855	−1.624
H	48	Q	−5.294	6.819	0.665
H	48	R	−2.546	5.670	−5.052
N	65	S	3.241	1.199	−0.813
D	76	V	−6.563	12.791	2.922
D	76	Y	−6.816	2.921	−1.19
G	93	A	−3.804	12.803	0.707
G	93	D	22.897	20	−0.728
G	93	R	33.12	20	−0.087
G	93	S	2.8	20	9.944
G	93	V	20.699	14.997	15.008
A	95	T	−15.237	16.537	−0.281
D	101	G	−0.759	4.967	−1.86
D	101	H	0.31	9.361	0.142
D	101	N	−8.335	−1.371	−1.119
D	101	Y	0.921	14.853	−1.064
I	104	F	19.486	20	6.935
S	105	L	−14.356	−7.769	−6.383
L	106	F	13.187	20	2.706
L	106	V	7.353	4.349	−2.924
I	112	M	−3.703	−7.888	−1.988
I	112	T	−4.586	6.172	2.826
G	114	A	−10.812	11.700	−1.375
R	115	G	−3.484	−0.425	0.439
V	118	L	2.858	8.345	−4.0
D	124	G	−6.602	7.756	−4.152
D	125	H	−6.848	5.791	−3.271
L	127	R	−2.293	20	24.563
S	134	N	−8.502	3.170	6.118
G	141	E	21.177	7.283	1.218
A	145	T	−8.669	5.199	4.399
G	147	R	24.122	20	20.585
V	148	G	1.548	13.447	−5.315
V	148	I	−11.136	−2.324	2.884

Predicted $\Delta\Delta G$ (in kilocalories per mole) for known ALS disease mutations on structures of the SOD1 trimer, dimer, and monomer. Dimer and monomer structures are from Protein Data Bank ID code 1SPD; trimer structure, as in the main text, is model 1 described in Dataset S1. We note that our identified mutations for stabilizing or destabilizing the SOD1 trimer are not known disease mutants, likely because we specially selected them to affect only the trimeric form of SOD1 and not the native monomer or dimer species, artificially limiting our choices. Our purpose in choosing such mutations was for clean, unambiguous results verifying the identity of residues in the trimer interfaces, whereas the disease is most likely caused by mutations that affect the stability of all forms of SOD1, including the native forms for which we deselect here. AA, amino acid; $\Delta\Delta G_D$, change in free energy upon mutation for the structure of SOD1 native dimer; $\Delta\Delta G_M$, change in free energy upon mutation for the structure of SOD1 native monomer; $\Delta\Delta G_T$, change in free energy upon mutation for the structure of SOD1 trimer.

Table S2. Human SOD1 limited proteolytic digest peptides identified by MS

Form of SOD	Observed	M_r(expt)	M_r(calc)	Peptide	Mascot assignment	Notes
V8 (100 mM phosphate, pH 4.0, t = 1 min)						
Monomer	No matches					First peptide identified at t = 5 min
Dimer	No matches					No peptides out to t = 10 min
Trimer	1,459.0857	1,458.0784	1,457.7514	D.GPVQGIINFEQKE.S	SOD1 G12-E24	
	2,396.6919	2,395.6846	2,395.1616	E.ERHVGDLGNVTADKDGVADVSIE.D	SOD1 E78-E100	
Chymotrypsin (100 mM Tris 50 mM $CaCl_2$, pH 7.8, t = 2 min)						
Monomer	No matches					First peptide identified at t = 10 min
Dimer	No matches					No peptides out to t = 10 min
Trimer	1,400.4094	1,399.4021	1,399.7096	F.EQKESNGPVKVW.G	SOD1 E21-W32	
	3,580.9929	3,579.9856	3,580.7904	L.VVHEKADDLGKGGNEESTKTGNA-GSRLACGVIGIAQ.-	SOD1 V118-Q153	
Pepsin (100 mM acetate, pH 3.5, t = 1 min)						
Monomer	1,244.4987	1,243.4914	1,243.6561	L.KGDGPVQGIINF.E	SOD1 K9-F20	
	2,696.9983	2,695.9910	2,696.3922	F.EQKESNGPVKVWGSIKGLTEGLHGF.H	SOD1 E21-F45	
Dimer	1,244.7208	1,243.7135	1,243.6561	L.KGDGPVQGIINF.E	SOD1 K9-F20	
	2,697.4995	2,696.4922	2,696.3922	F.EQKESNGPVKVWGSIKGLTEGLHGF.H	SOD1 E21-F45	
Trimer	1,244.6426	1,243.6353	1,243.6561	L.KGDGPVQGIINF.E	SOD1 K9-F20	

We used three proteases with different specificity: V8 cuts after D and E; chymotrypsin cuts after F, W, Y, H, M, and L (unless followed by P); and pepsin cuts before L, F, W, and Y (unless preceded by P). Buffer, pH, and digest time are listed for each limited proteolytic reaction with the purified SOD1 monomer, dimer, or trimer. SOD1 monomer and dimer required longer digest times with V8 or chymotrypsin to observe proteolytic cleavage products; we collected time points of proteolytic cleavage reactions out to t = 10 min. Notably, we did not observe proteolytic cleavage of the SOD1 dimer with V8 or chymotrypsin even after 10 min of incubation, in agreement with the known highly stable structure of the native SOD1 dimer. M_r(calc) is the calculated molecular mass from the matched peptide sequence, M_r(expt) is the experimental *m/z* transformed to a relative molecular mass, and Observed is the experimental *m/z* from the mass spectrometer. Definitions are from Matrix Science (www.matrixscience.com/help/pmf_summaries_help.html#PROTSUM).

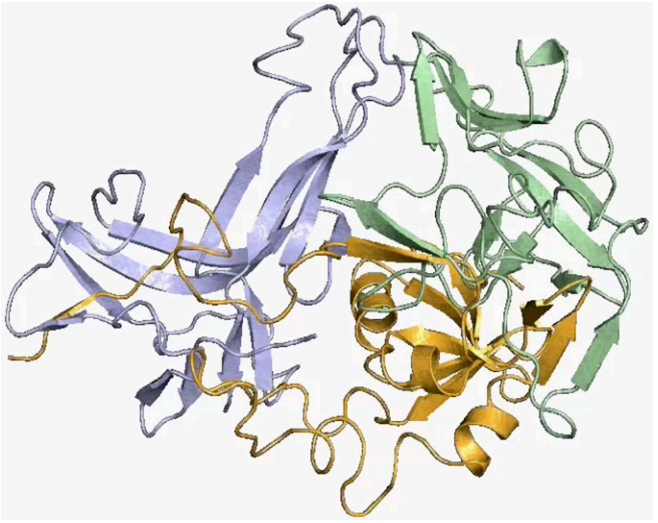

Movie S1. SOD1 trimer model. A 360° view of the SOD1 trimer model is shown in cartoon representation. Each monomer is represented in a different color: pale green, bright orange, and light blue.

Movie S1

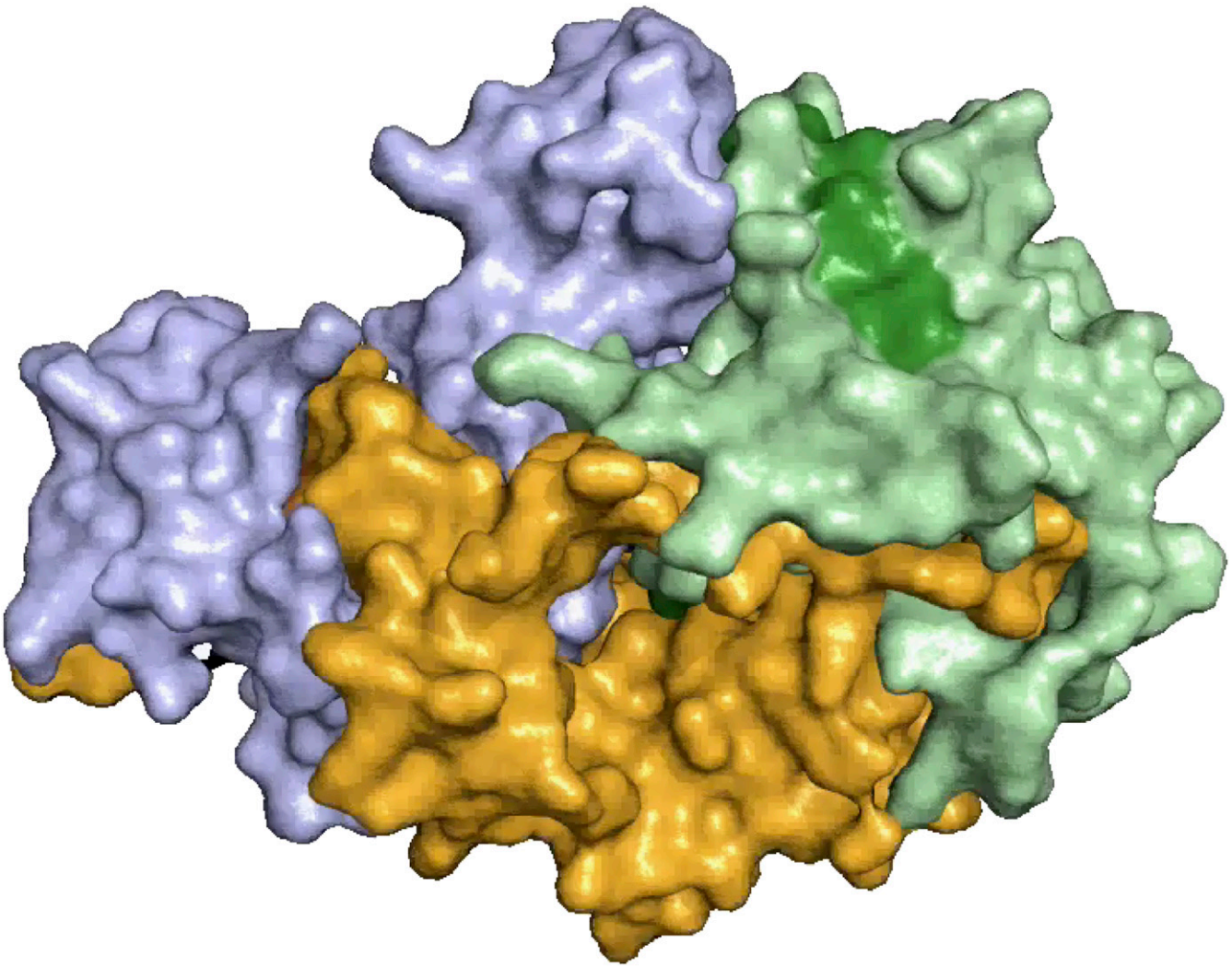

Movie S2. Monomer–monomer interfaces of the SOD1 trimer differ from the native dimer interface. A 360° view of the SOD1 trimer model is shown in surface representation. Each monomer is represented in a different color: pale green, bright orange, and light blue. The residues comprising the native dimer interface are highlighted in darker colors: forest, brown, and deep blue, respectively. We note that the native dimer interfaces are solvent-exposed and separated in discrete patches across the surface of the SOD1 trimer.

Movie S2

Other Supporting Information Files

Dataset S1 (PDF)